Electronic Supplementary Material (ESI) for Journal of Materials Chemistry A.

Supporting Information

Efficient and stable charge transfer channels for photocatalytic water splitting activity of CdS without sacrificial agents

Wei Chen,[a] Guo-Bo Huang,*[a] Hao Song,[b] and Jian Zhang*[b,c]

a. School of Pharmaceutical and Materials Engineering, Taizhou University, Taizhou, 318000, Zhejiang Province, PR China. Email: gbhuang973@163.com

b. New Energy Technology Engineering Lab of Jiangsu Province, School of Science, Nanjing University of Posts & Telecommunications, Nanjing 210023, PR China. Email: iamjzhang@njupt.edu.cn

c. Key Laboratory for Organic Electronics and Information Displays & Institute of Advanced Materials (IAM), Jiangsu National Synergetic Innovation Center for Advanced Materials (SICAM), Nanjing University of Posts & Telecommunications, Nanjing 210023, PR China.

Experimental

Chemicals

All chemicals were used as received. Cadmium nitrate tetrahydrate ($Cd(NO_3)_2{\cdot}4H_2O$, 99.9%), sodium diethyldithiocarbamate ($NaS_2CN(C_2H_5)_2$, 99%), bis(cyclopentadienyl)nickel ($C_{10}H_{10}Ni$, 98%), dichloromethane (CH_2Cl_2, 99.9%) and trichloromethane ($CHCl_3$, 99.9%) were purchased from Aladdin.

Deposition of CdS nanorods arrays

CdS nanorods arrays were synthesized according to our previous literature reports. In a typical process, 380 mg of the precursor ($Cd(S_2CN(C_2H_5)_2)_2$) from the mixture of the $Cd(NO_3)_2{\cdot}4H_2O$ and $NaS_2CN(C_2H_5)_2$ solutions (mol% 1:1.2) was dissolved in 20 mL mixture of CH_2Cl_2 and $CHCl_3$ (vol% 1:1) in a three-necked round-bottomed flask (50 mL). The carrier gas (Ar) was passed into the solution to transport the aerosol which from a water bath above the piezoelectric modulator of a PARKOO ultrasonic humidifier (Model YDH803EB). FTO glass (1 × 2 cm) was placed into the reactor tube of a furnace (CARBOLITE). Thus, the aerosol droplets of the precursor generated were transferred into the hot wall zone of the reactor by Ar. Deposition was carried out at 400 ℃ for 50 min.

Deposition of CdS/NiOOH Core/Shell heterojunctions

The NiOOH was deposited on the CdS arrays electrodes through Savannah S100 ALD reactor (Ultratech Inc.). The CdS film electrodes were deposited into the reaction chamber of ALD at 120 °C with a continuous N_2 flow rate of 10 sccm. $C_{10}H_{10}Ni$ (100 °C) and O_3 provided Ni and O sources, respectively. The deposition consisted of a 1 s pulse of $C_{10}H_{10}Ni$ with a 5 s exposure and an 8 s purge, and a 1 s pulse of O_3 with a 5 s exposure and 3 s purge, repeated to obtain the desired thickness. According to the deposition thickness, the samples were named as CdS (without NiOOH), CdS/2NiOOH (NiOOH with 2 nm thickness), CdS/4NiOOH (NiOOH with 4 nm thickness) and CdS/16NiOOH (NiOOH with 16 nm thickness), respectively. Electrodes were removed from the reaction chamber at 120 °C.

Characterization

The X-ray diffraction (XRD) was carried out on a D8 Advance X-ray powder diffractometer with Cu Ka radiation with a scan speed of 0.5 s per step. The morphologies of the samples were characterized by transmission electron microscopy (TEM) (FEI Tecnai F20) at an acceleration voltage of 200 kV. Scanning transmission electron microscopy (STEM) was performed using a FEI Titan 80-200 (ChemiSTEM) electron microscope operated at 200 kV, equipped with a high angle annular dark field (HAADF) detector, while compositional maps were obtained with energy dispersive spectroscopy (EDS) using four large solid-angle symmetrical Si drift detectors. The scanning electron microscopy (SEM) images were obtained on a scanning electron microscope (Hitachi S-4800). The X-ray photoelectron spectra images (XPS) were performed on a ESCALAB 250i X-ray photoelectron spectrometer monochromatic Al Kα radiation. The electron paramagnetic resonance (EPR) spectrum was monitored using a digital X-band spectrometer (EMX-220, Bruker). Inductively coupled plasma atomic emission spectrometry (ICP-AES) analysis was performed on a Thermo ICAP-6300 instrument (USA). The femtosecond time-resolved transient absorption (fs-TA) spectroscopy was employed to reveal the dynamics of the four photocatalysts (CdS, CdS/2NiOOH, CdS/4NiOOH and CdS/16NiOOH) in Nafion (5% w/w in water and 1-propanol). All samples were pumped at 400 nm with a 1 kHz repetition rate at a fluence of 2.95 μJ cm^{-2} through a Clark MXR CPA-2001 laser. The CPA-2001 has a 150 fs pulse duration with a fundamental output wavelength of 780 nm, 5% of which is frequency doubled to 390 nm using a BBO crystal to create the pump beam.

Photoelectrochemical (PEC) measurements

The photocurrent density was measured on a CHI 660D electrochemical station (Shanghai Chenhua, China) in ambient conditions. A standard three-electrode setup was used with the as-deposited electrodes as working electrode (catalyst coverage area: 1 cm × 1 cm), a Pt foil as counter electrode, and a Ag/AgCl electrode as reference electrode. The three electrodes were inserted in a quartz cell filled with 0.5 M Na_2SO_4 electrolyte for photocurrent measurements. An AM 1.5G filter was used to obtain one sun light intensity (100 mW cm^{-2}). IPCE measurements were performed on CdS/4NiOOH and CdS at 1.23 V *vs*. RHE. The computational formula of IPCE is as follows:

$$\mathrm{IPCE} = 1240\ I / (\lambda \times J_{light})$$

Where λ, I and J_{light} mean wavelength of incident light, photocurrent density and irradiation intensity of 100 mW/cm^2, respectively.

Photocatalytic hydrogen production measurements

Photocatalytic hydrogen evolution experiments were carried out at a constant temperature (25 °C) in a closed gas circulation system. A 300 W Xe lamp (91160, Newport, USA) equipped with a UV-light cut-off filter ($\lambda \geq 420$ nm) was used to provide visible light. The dry powder samples were scraped from the FTO glass firstly. In a typical experiment, 20 mg of photocatalyst was dispersed in 150 mL of deionized water. The H_2 content was analyzed using an online gas chromatography (equipped with a TCD detector) with argon as the carrier gas. The apparent quantum efficiency (QE) plotted were estimated though several cut-off filters, and were calculated on the basis of the number of the incident photons in each wavelength region. Accordingly, each value is plotted in the middle of two cut-off wavelengths. The apparent QE was calculated according to equation:

$$\begin{aligned}\mathrm{QE}[\%] &= \frac{\text{number of reacted electrons}}{\text{number of incident photons}} \times 100 \\ &= \frac{\text{number of evolved } H_2 \text{ molecules} \times 2}{\text{number of incident photons}} \times 100\end{aligned}$$

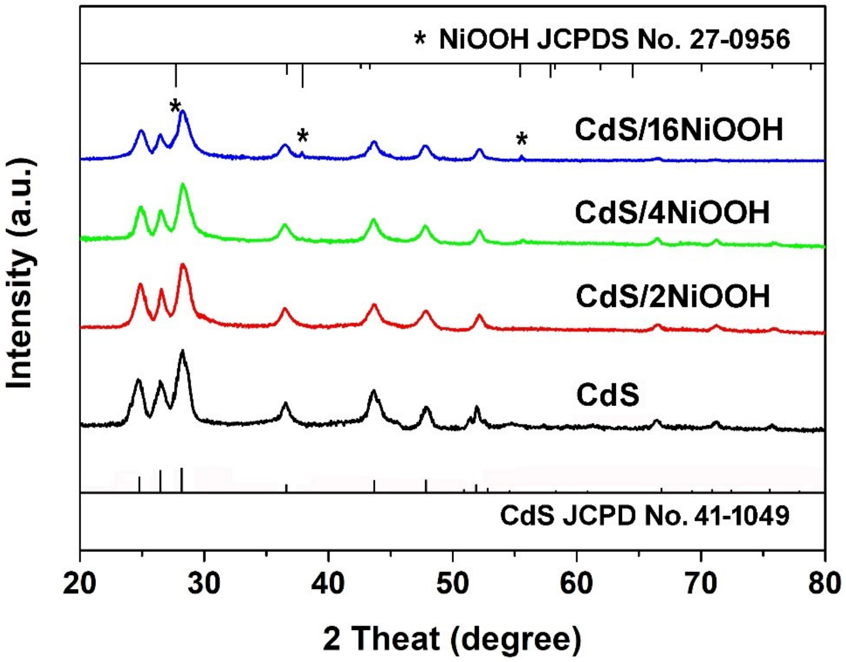

Fig. S1 XRD patterns of CdS, CdS/2NiOOH, CdS/4NiOOH and CdS/16NiOOH.

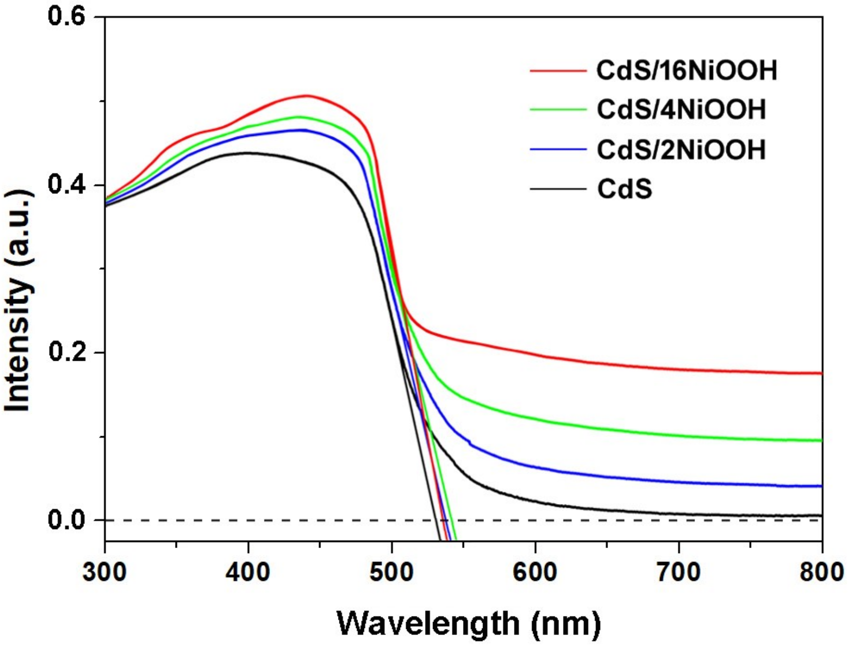

Fig. S2 UV-vis absorption spectra of CdS, CdS/2NiOOH, CdS/4NiOOH and CdS/16NiOOH.

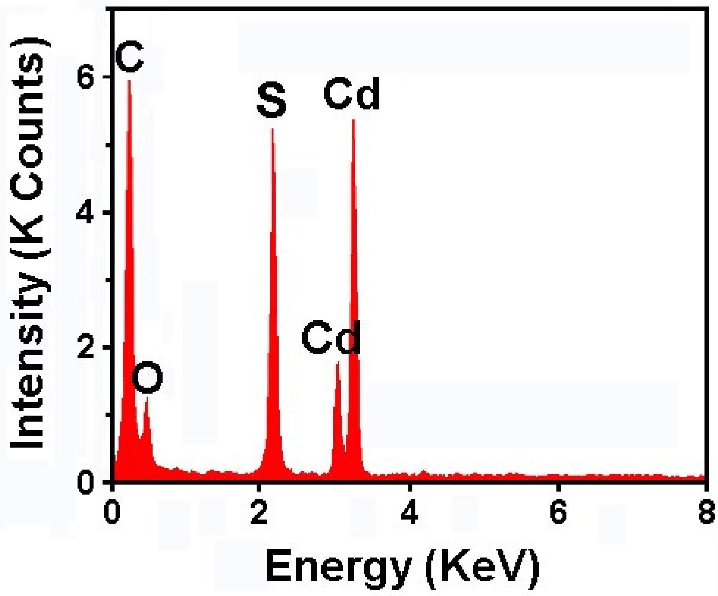

Fig. S3 EDS pattern of CdS.

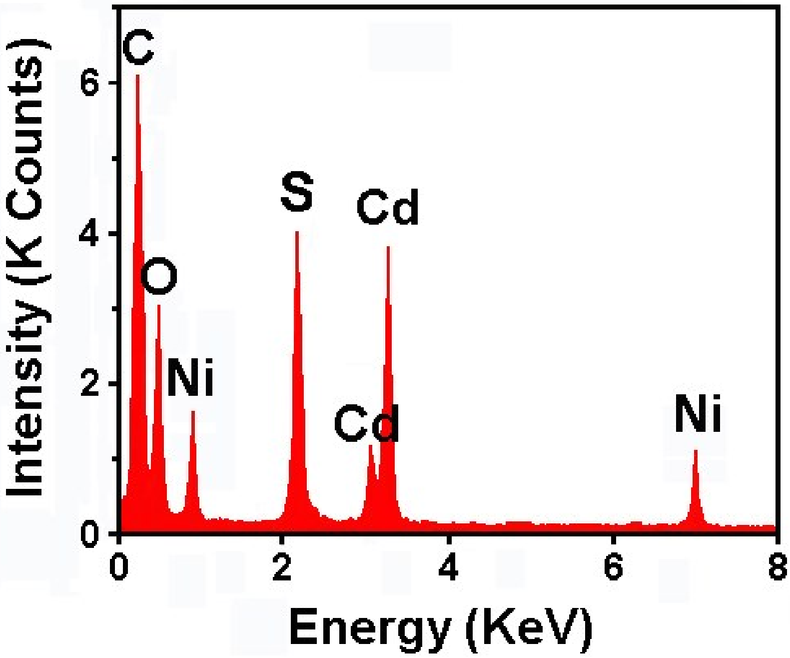

Fig. S4 EDS pattern of CdS/16NiOOH.

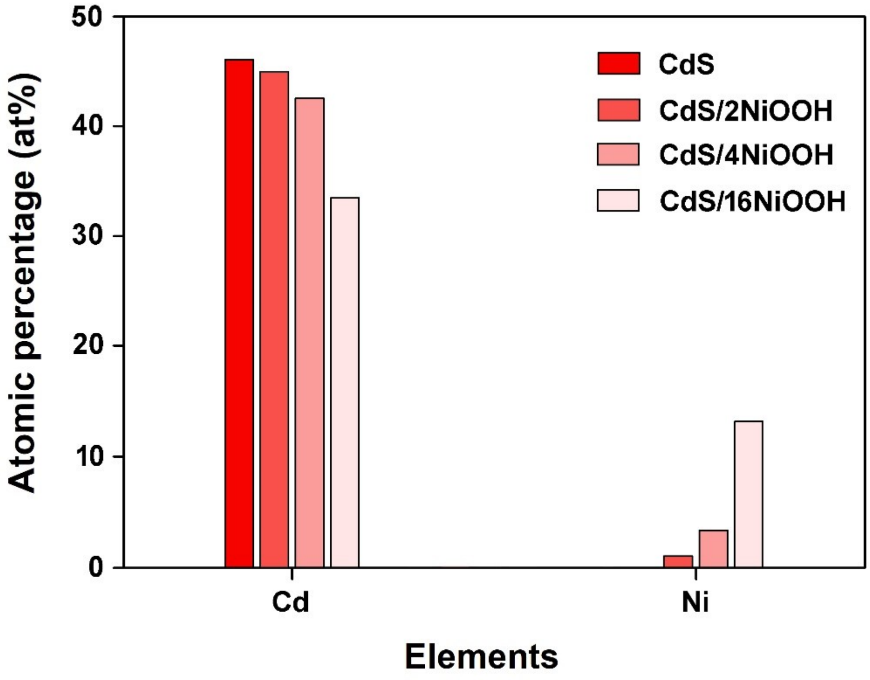

Fig. S5 ICP-AES of Cd and Ni over CdS, CdS/2NiOOH, CdS/4NiOOH and CdS/16NiOOH.

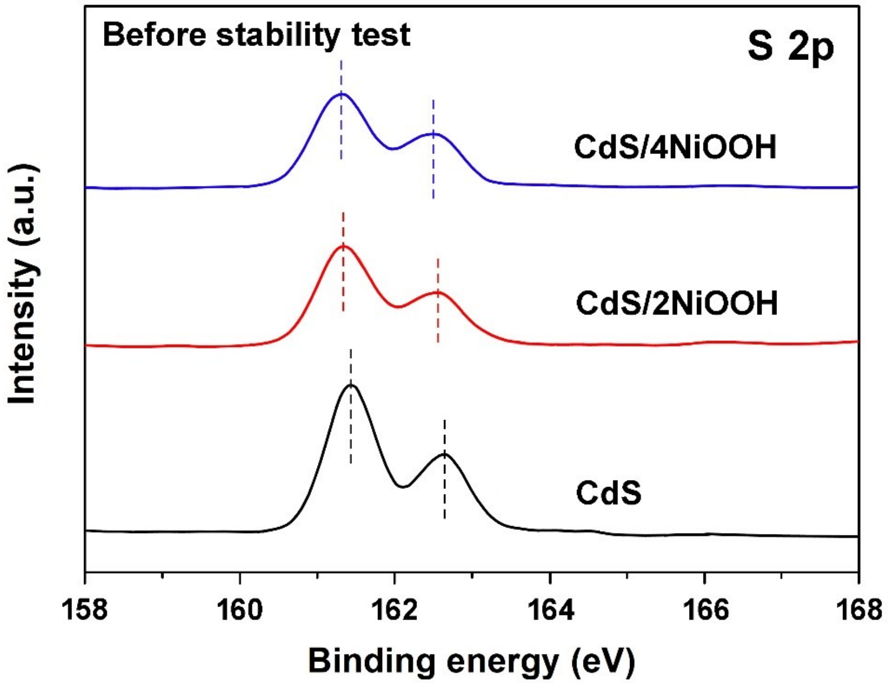

Fig.S6 High-resolution XPS for S 2p of CdS, CdS/2NiOOH and CdS/4NiOOH.

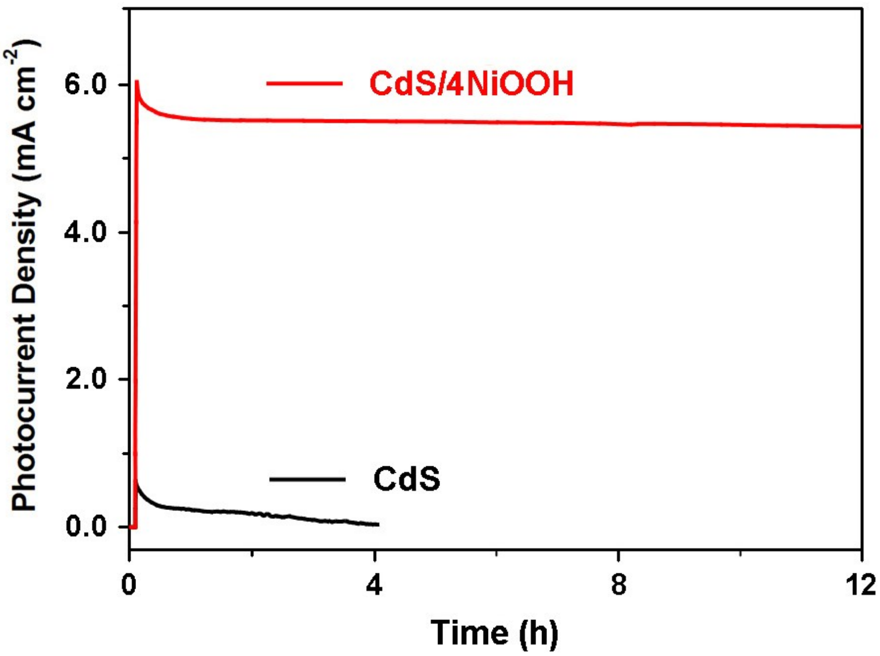

Fig. S7 Photocurrent stability of CdS and CdS/4NiOOH under continuous illumination for 12 h.

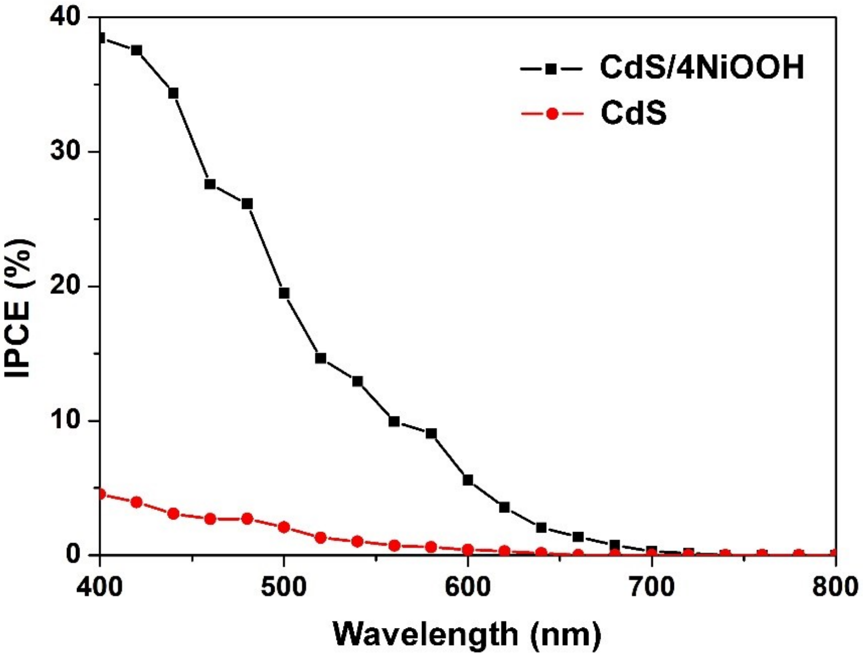

Fig. S8. IPCE spectra of CdS and CdS/4NiOOH at 1.23 V *vs*. RHE.

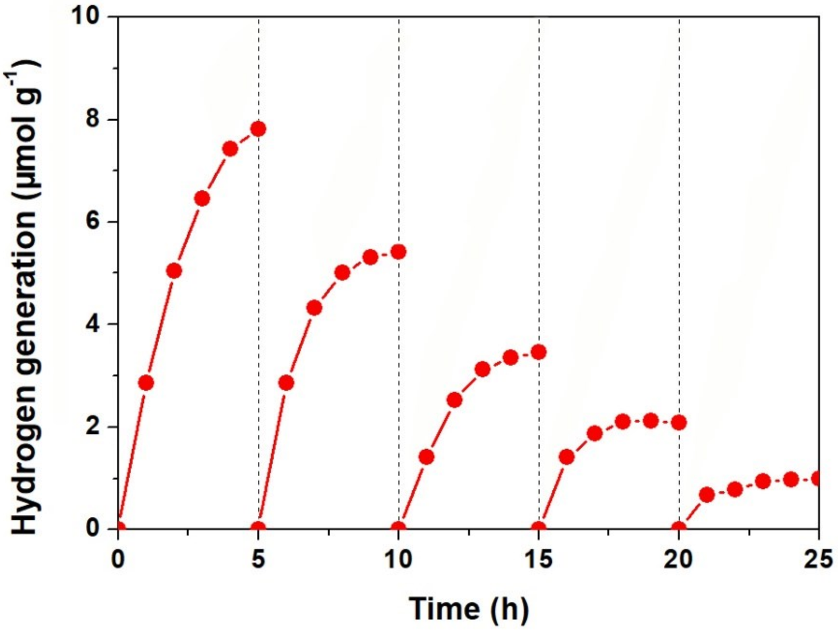

Fig. S9 Cycling tests of photocatalysis hydrogen generation over CdS under visible light irradiation.

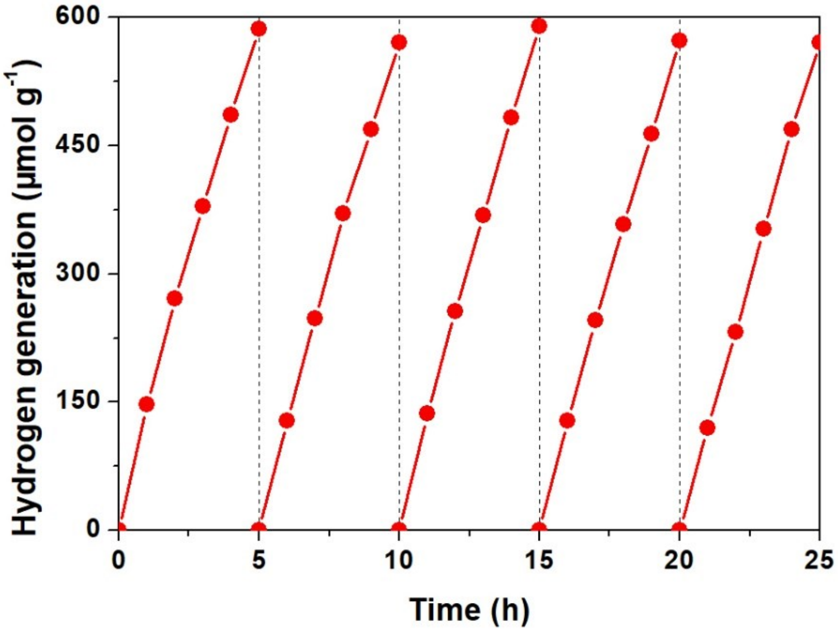

Fig. S10 Cycling tests of photocatalysis hydrogen generation over CdS/4NiOOH under visible light irradiation.

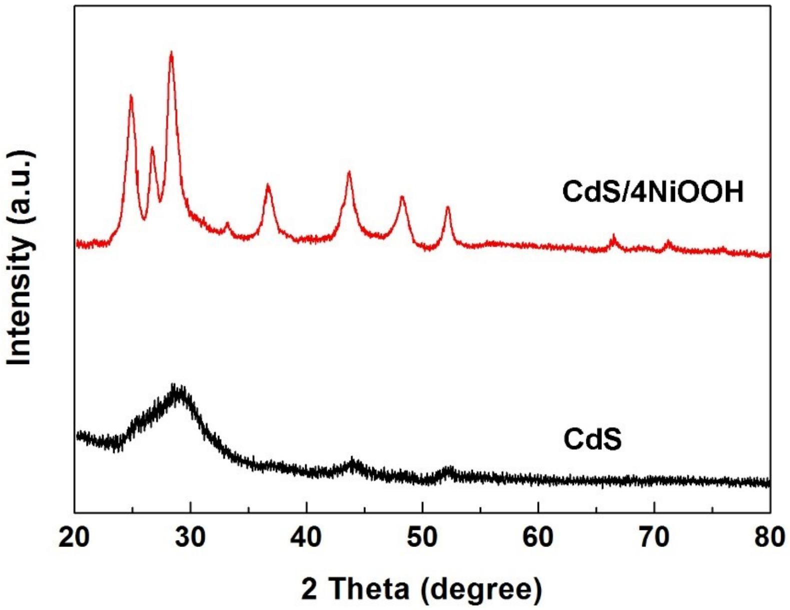

Fig. S11 XRD patters of CdS and CdS/4NiOOH after photostability tests (25 h).

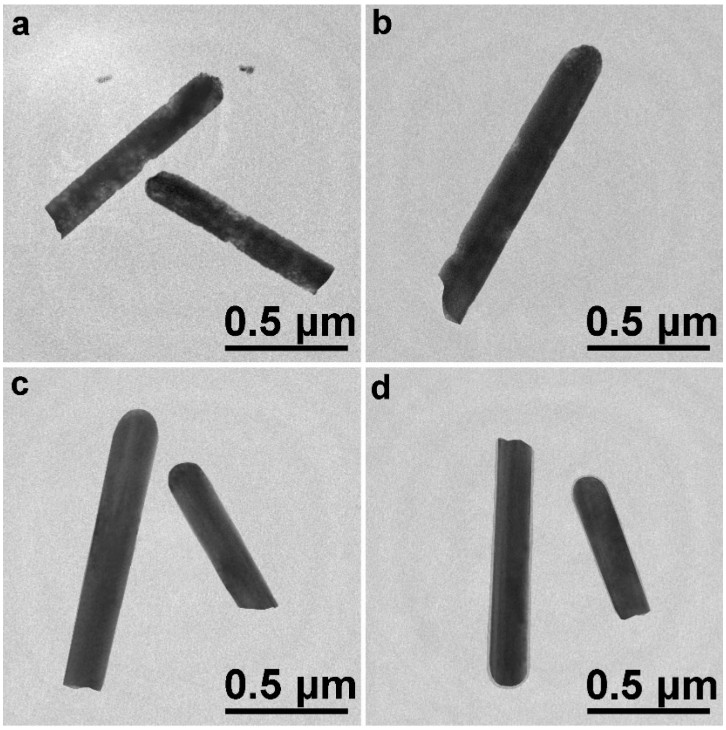

Fig. S12 TEM images of CdS (a), CdS/2NiOOH (b), CdS/4NiOOH (c) and CdS/16NiOOH (d) after photostability tests (25 h).

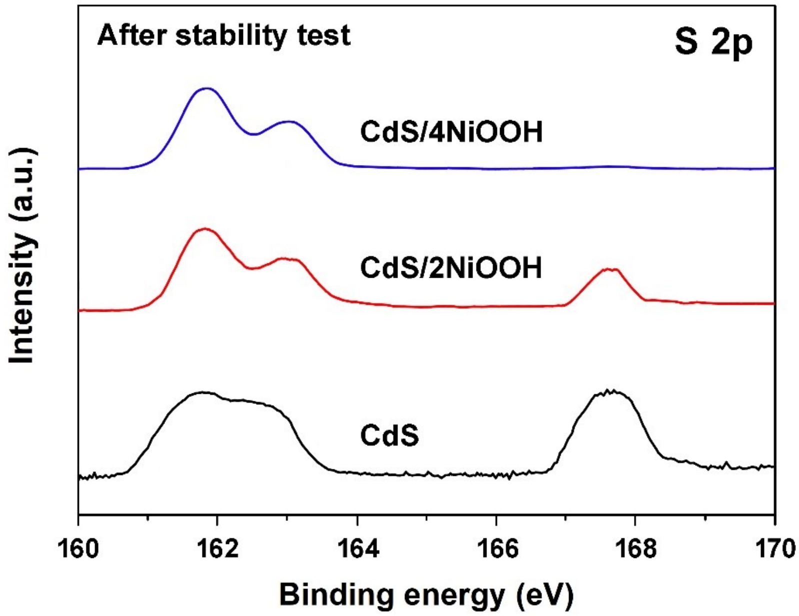

Fig. S 13 S 2p XPS of CdS, CdS/2NiOOH and CdS/4NiOOH after photostability tests (25 h).

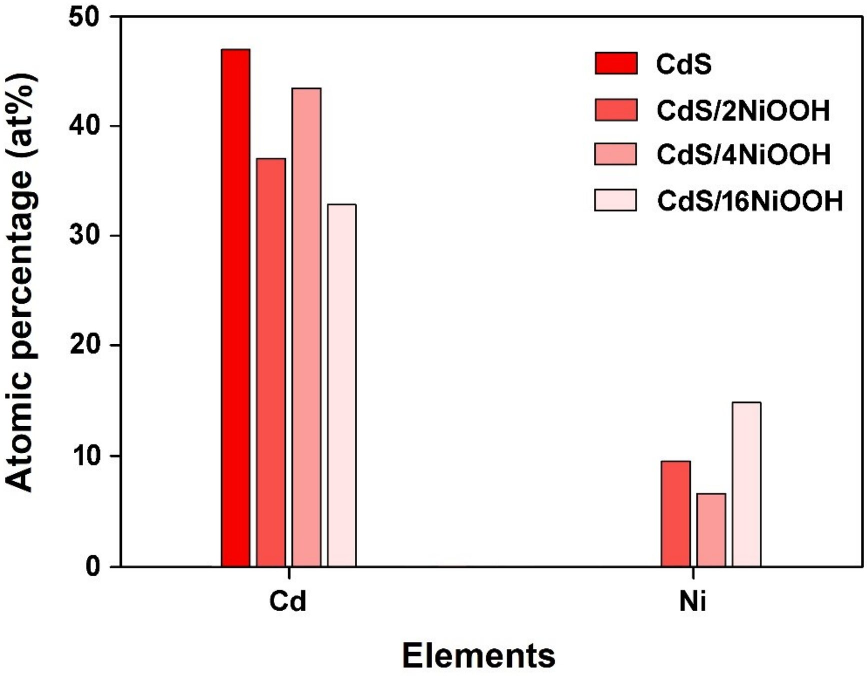

Fig. S14 ICP-AES of Cd and Ni over CdS, CdS/2NiOOH, CdS/4NiOOH and CdS/16NiOOH after photostability test.

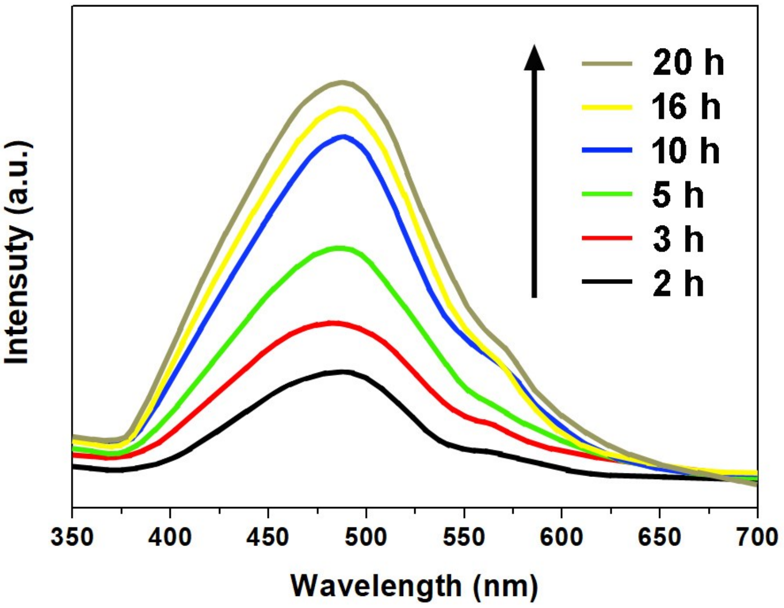

Fig. S15 Time dependence of the absorption intensity of H_2O_2 over the CdS/4NiOOH suspension during photocatalytic water splitting; the content of H_2O_2 was measured by UV-vis spectrophotometry. In an acidic environment, Fe^{2+} can be oxidized into Fe^{3+} by H_2O_2, and Fe^{3+} can be combined with KSCN to form $[Fe(SCN)]^{2+}$. $[Fe(SCN)]^{2+}$ has the maximum absorption peak at 475 nm.

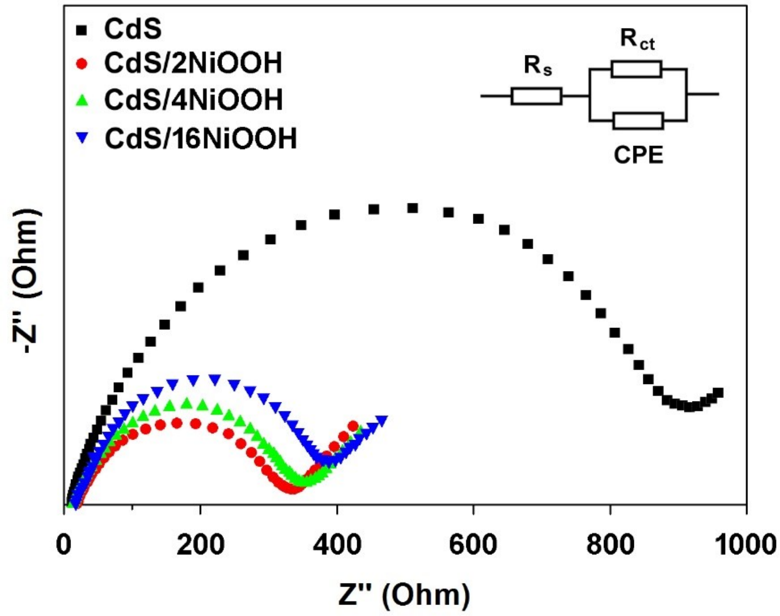

Fig. S16 EIS patterns of CdS, CdS/2NiOOH, CdS/4NiOOH and CdS/16NiOOH electrodes.

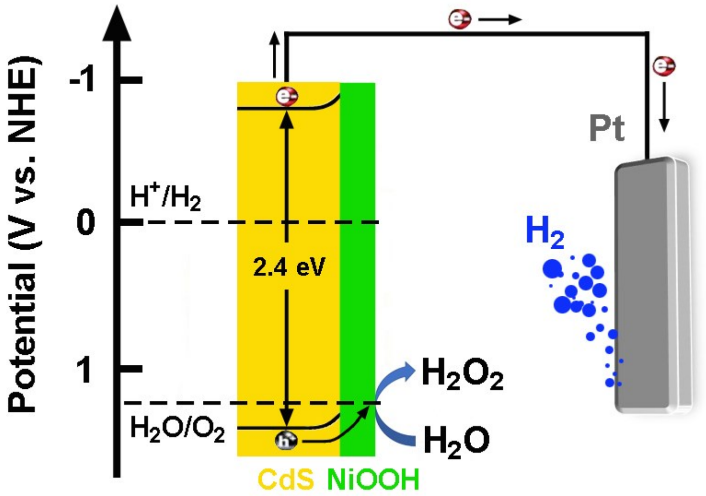

Fig. S17 Cross-sectional schematic and energy band alignment of the prepared hybrid.

Table S1 Comparison of the visible light photocatalytic activity for several recently reported CdS with different protection coatings.

Catalysts	**Protection coatings**	**H_2 generation rate (μmol h^{-1} g^{-1})**	**Stability (h)**	**Reference**
CdS	**NiOOH**	**118.6**	**25**	**This work**
CdS	MnO_2/NiSe	455.0	24	*J. Catal.*, 2018, **367**, 269-282.
CdS	WO_3/Pt	186.2	24	*J. Catal.*, 2017, **350**, 189-196.
CdS	Al_2O_3/Pt	62.1	30	*Appl. Catal. B Environ.*, 2018, **226**, 373-383.
CdS	TiO_2/Pt	3.074	10	*Appl. Catal. B Environ.*, 2017, **212**, 129-139.
CdS	Cr_2O_3/Pt	63.3	8	*Appl. Catal. B Environ.*, 2018, **221**, 618-625.
CdS	Ni_2P	837.94	12	*Appl. Catal. B Environ.*, 2018, **221**, 243-257
$Zn_{0.8}$ $Cd_{0.2}S$	NiO	99.9	12	*ChemSusChem*, 2019, **12**, 1410-1420